Influence of the absorption grating on the diffraction efficiency in thick photovoltaic media in transmission geometry under non linear regimes

L.M. Cervantes[a], A. Zúñiga[b], L.F. Magaña[c,*], and J.G. Murillo[d]
[a]*Escuela Superior de Cómputo, Instituto Politécnico Nacional, Unidad Profesional Adolfo López Mateos, México D.F., 07730 México.*
[b]*Escuela Superior de Física y Matemáticas, Instituto Politécnico Nacional, Edificio 9, Unidad Profesional Adolfo López Mateos, México D.F., 07730 México.*
[c]*Instituto de Física, Universidad Nacional Autónoma de México, Apartado Postal 20-364, México D.F., 01000 México.*
[d]*Centro de Investigación en Materiales Avanzados, Miguel de Cervantes 120, Complejo Industrial Chihuahua, 31109 Chihuahua, México.*

Recibido el 29 de abril de 2010; aceptado el 25 de mayo de 2010

With simultaneous phase and absorption gratings, we calculated the contribution of the absorption grating to the total diffraction efficiency in thick samples ($\approx$ 1 cm) of iron doped $LiNbO_3$. We considered transmission geometry, with an applied field of 5 kV/cm. First we solved numerically the set of partial, non linear, material rate differential equations. These solutions were used to calculate the energy exchange in two wave mixing. We solved numerically the beam coupling equations along sample thickness, for different values of grating period. For the used value of iron doping, we found that the contribution of the absorption grating is less than 0.02% of the total value of the diffraction efficiency.

Keywords: Photorefractive gratings; absorption gratings; diffraction efficiency; non linear optics.

Con rejillas simultáneas de fase y de absorción, calculamos la contribución de la rejilla de absorción a la eficiencia total de difracción en muestras gruesas ($\approx$1 centimetro) de LiNbO3 dopado con hierro. Consideramos la geometría de transmisión, con un campo aplicado de 5 kV/cm. Primero resolvimos numéricamente el sistema de ecuaciones diferenciales parciales, no lineales del material. Estas soluciones fueron utilizadas luego para calcular el intercambio de energía en la mezcla de dos ondas. Resolvimos numéricamente las ecuaciones del acoplamiento de los haces a lo largo del grosor de la muestra, para diversos valores del período de la rejilla. Para el valor usado del dopaje de hierro, encontramos que la contribución de la rejilla de absorción es menos de 0.02 $\%$ del valor total de la eficiencia de difracción.

Descriptores: Rejillas fotorrefractivas; rejillas de absorción; eficiencia de difracción; óptica no lineal.

PACS: 42.65.-k; 42.70-a; 42.70.Nq

1. Introduction

Ferroelectric lithium niobate is a photorefractive material that has attracted a great deal of research interest. This material is a photovoltaic medium that has a great optical quality and excellent photorefractive properties. It is widely used for electro-optic modulators and frequency doublers. It has been used in a large variety of optical devices [1-5]; for this reason this material's properties are of special interest. In this work, we are interested on the relevance of the absorption grating on the value of the total diffraction efficiency for transmission gratings of iron doped lithium niobate.

The absorption grating appears because of the redistribution of electrons between the ionized and un-ionized donors. The absorption coefficient is proportional to the non ionized donors, which are available for ionization [6,7]. From this and from the numerical solution to the material rate equations, we have obtained an expression for the absorption modulation and its phase.

For strong beam coupling there is a spatial redistribution of the light intensity pattern. In this way, the grating is spatially non-uniform and its amplitude and phase become a function of crystal thickness. The uniform grating approximation is reasonable for weak coupling or thin-enough crystals. It is not adequate for fiber like crystals [8], or for strong coupling and high modulation depth [9].

We considered thick samples and high modulation depths. Under these conditions, we have strong beam coupling effects. We also considered the grating vector, K_G, of the recorded spatial grating directed along the crystal axis and parallel to the external field E_0, as shown in Fig. 1. We started by solving numerically the set of non-linear material rate differential equations for $LiNbO_3$ to find the full overall space charge field, from $t = 0$ seconds up to the stationary state. After that, we used these solutions to calculate the absorption modulation and phase and the diffraction efficiency for two wave mixing, including the non uniformity of the grating, and of the magnitude and phase of the light modulation along sample thickness.

2. Theoretical framework

We restrict our consideration to the band-transport model. We consider only one type of charge carriers (electrons) and one photoactive impurity level [10]. The differential equations in this model are the following.

TABLE I. Experimental parameters [4,11-12] for $LiNbO_3$ taken for our calculations.

	Iron doped $LiNbO_3$		Ref.
ε	Dielectric constant	30	[11]
n	Average refractive index	2.34	[11]
r_{eff}	Electro optic coefficient (mV^{-1})	8.6×10^{-12}	[11]
Λ	Fringe spacing (nm)	105	
μ	Mobility lifetime product ($cm^2\ V^{-1}$)	810^{-5}	[11]
γ	Recombination constant (m^3s^{-1})	5.0×10^{-14}	[11]
β	Thermal-excitation rate	0	
s	Photo ionization cross section (m^2J^{-1})	9.7×10^{-5}	[12]
$s\kappa$	Photovoltaic coefficient ($cm^3\ V^{-1}$)	1.56817×10^{-26}	[12]
E_{ph}	Photovoltaic field (V/cm)	1.0×10^4	[11]
N_D	Donor density ($m^{-3)}$	10^{26}	[4]
N_A	Acceptor density (m^{-3})	10^{24}	[4]
α_0	Absorption coefficient (cm^{-1})		
	$\lambda = 488$ nm	3.0	[4]

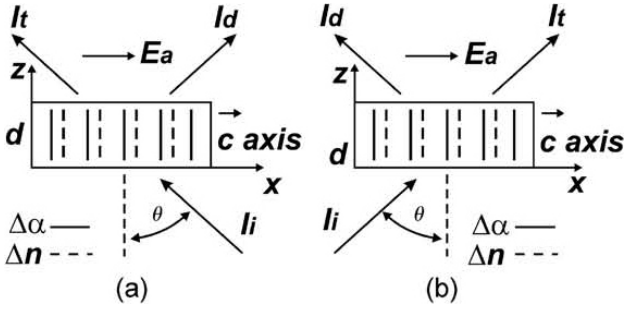

FIGURE 1. Transmission geometry; θ is the angle of incidence. I_{inc} is the incident beam; I_t and I_d are the transmitted and diffracted beams respectively; In a) the incident beam comes from the right; in b) the incident beam comes from the left; the sample thickness is d. The applied field is E_0.

$$\frac{\partial N_D^+}{\partial t}=(\beta+sI)(N_D-N_D^+)-\gamma n N_D^+, \tag{1}$$

$$\rho=\frac{\partial(\varepsilon_0\varepsilon E_{SC})}{\partial z}, \tag{2}$$

$$\rho=e(N_D^+-N_A-n), \tag{3}$$

$$j=e\mu n(E_{SC}+E_0)+\mu k_B T\frac{\partial n}{\partial z}+pI(N_A-N_D^+), \tag{4}$$

$$\frac{\partial \rho}{\partial t}=-\frac{\partial j}{\partial z}\ . \tag{5}$$

Where N_A, N_D, N_D^+ and n are respectively the densities of compensating acceptors centers, donors, ionized donors and free electrons; s is the light-excitation cross section, γ is the two-body recombination coefficient; β is the thermal-excitation rate; ε is the static dielectric constant, μ is the electron mobility; k_B is the Boltzmann's constant; T is the absolute temperature; E_0 is the external homogeneous electric field; E_{SC} is the space-charge field; e is the elementary charge and p is the photovoltaic coefficient. The experimental parameters [11-12] used for $LiNbO_3$ are shown in Table I.

The light excites electrons to the conduction band. These electrons migrate due to diffusion, drift and photovoltaic effect. This migration is from the bright to the dark parts of the crystal where they are captured by the compensating centers. In this manner a space charge field appears.

The illumination on the sample is the following.

$$I(\vec{r}) = I_0\left(1+\frac{m}{2}\exp(\vec{K}_G\bullet\vec{r}-\delta) + \frac{m*}{2}\exp(-i(\vec{K}_G\bullet\vec{r}-\delta))\right)\ . \tag{6}$$

Where δ refers to the phase difference between the incident waves, m is the complex light modulation.

$$m(\vec{r}) = \frac{2A_1(\vec{r})A_2^*(\vec{r})}{I_0(\vec{r})} = \left|m(\vec{r})\right|\exp(i\psi_m(\vec{r})), \tag{7}$$

And; $\vec{K}_G=\vec{k}_1-\vec{k}_2$; $\vec{k}_1$, $\vec{k}_2$ are the incident wave vectors.

When a sinusoidal illumination pattern is recorded on the crystal, the optical properties of the medium vary in a harmonic way.

$$n = n_0 + n_1\cos(\vec{K}_G\bullet\vec{r}+\Phi_G+\psi_m). \tag{8}$$

The absorption coefficient is

$$\alpha(\vec{r}) = \alpha_0 + |\alpha_1|\cos(\vec{K}_G\bullet\vec{r}+\varphi_a). \tag{9}$$

Where $\vec{K_G}$ is the grating vector, which is perpendicular to the fringes recorded in the medium; n is the refractive index of the medium at the point $\vec{r}$; n_0 is the average refractive index and n_1 is the refractive modulation, ψ_m is the phase of the complex light modulation, $m(z)$; Φ_G is the phase of the photorefractive grating; $\alpha(\vec{r})$ is the absorption at the point $\vec{r}$; α_0 is the average absorption; α_1 is the absorption modulation and φ_a is the phase of the absorption grating.

We solved numerically the set of non-linear material rate differential equations (1)-(5), for a fringe spacing $\Lambda = 0.250$ microns. We obtained the overall space charge field. We followed the method described elsewhere [13,14]. We then obtained the numerical solutions for several values of $m_0 = |m(z=0)|$, that is the absolute value of the complex light modulation at the surface of the sample, between 0 and 1, when recording. Then we performed the Fourier decomposition for the calculated overall space charge field. In this way, we obtained the amplitude E_1 , of its fundamental component and its phase, Φ_G, with regard to the light interference pattern. We did this for every one of the considered cases. We performed these calculations for an applied d.c. field of 5 kV/cm. It is necessary to mention that this method does not rely on a Fourier expansion so its validity

is not limited to using a truncated harmonic basis. In this way we have obtained the grating strength and its phase as functions of light modulation. These are necessary to solve, self-consistently, the beam coupling equations.

3. Coupled beam equations

Let the complex electric fields of the two beams interacting in the crystal be the following.

$$\psi_1 = A_1 \exp i(\omega t - \vec{k_1} \bullet \vec{r}) \tag{10}$$

$$\psi_2 = A_2 \exp i(\omega t - \vec{k_2} \bullet \vec{r} - \delta). \tag{11}$$

Where A_1 and A_2 are the complex amplitudes of the two beams; ω is the angular frequency. Equation (6) gives the intensity of the interference pattern inside the crystal.

We have also considered the absorption as given in Ref. 6,

$$\alpha(z) = S(N_D - N_D^+(z)). \tag{12}$$

Where N_D^+ is the ionized donor density [6]. We performed the Fourier decomposition of α(z) to obtain the amplitude of the absorption grating, $|\alpha_1|$, and its phase, φ_a. Then, we used these values in Eq. (9).

In the transmission geometry, the coupled beam equations are the following [15].

$$\frac{dA_1}{dz} = -i\left(\kappa^* - i\frac{b^*}{2}\right)A_2 - \frac{\alpha_0}{2}A_1, \tag{13}$$

$$\frac{dA_2}{dz} = -i\left(\kappa - i\frac{b}{2}\right)A_1 - \frac{\alpha_0}{2}A_2. \tag{14}$$

Where the coupling factor, κ is due to the space charge field; we calculated this factor from the solution of the material rate equations; it is complex, and changes along sample thickness, z.

$$\kappa = \frac{\pi \Delta n_1(z)}{\lambda \cos\theta} = \frac{\pi}{\lambda \cos\theta}\frac{n^3 r_{eff}\,|E_1(z)|}{2}\exp i(\Phi_G + \psi_m). \tag{15}$$

Where λ, θ, α and r_{eff} are the wavelength, the incidence angle, the absorption coefficient and the electro-optic coefficient, respectively. The coupling factor b is due to the absorption grating. It is:

$$b = i\,|\alpha_1| \exp(i\varphi_a) \tag{16}$$

The amplitude of the modulation of the absorption coefficient is:

$$|\alpha_1| = \alpha_0 \frac{N_{D1}^+}{(N_D - N_A)}. \tag{17}$$

Where N_{D1}^+ is the magnitude of the first Fourier coefficient of N_D^+. We obtained Eq. (17) using first the spatial average of α(z) over a grating period; then, we used the magnitude of the first Fourier coefficient of α(z). Notice that the spatial average of α(z) is α_0 and that the spatial average of $N_D^+(z)$ is N_A.

The solutions to the beam coupling Eqs. (13) to (14) must be self-consistent. This is because the changes in the intensities and phases of the waves cause changes on the light modulation and on the refraction index. These changes, in turn, induce new changes in the intensity and phases of the waves. We solved this set of equations in a self-consistent way. We considered no restrictions on the magnitude of the coupling factors given in Eqs. (15) and (16). We divided the sample in thin layers of thickness Δz [13] in such a way that within each layer $\kappa(z)$ is practically constant. This means that we did not allow $\kappa(z)$ to change more that 0.1% within each layer. In this way, within each layer we have analytical solutions

$$A_1 = \frac{i\beta}{2\kappa - ib}\left[C_1 \exp(\frac{1}{2}\beta z) - C_2 \exp(-\frac{1}{2}\beta z)\right] \times \exp(-\frac{1}{2}\alpha_0 z), \tag{18}$$

$$A_2 = \left[C_1 \exp(\frac{1}{2}\beta z) + C_2 \exp(-\frac{1}{2}\beta z)\right] \times \exp(-\frac{1}{2}\alpha_0 z), \tag{19}$$

Where

$$\beta = \sqrt{2i\,(b^*\kappa + \kappa^* b) + |b|^2 - 4\,|\kappa|^2},$$

C_1 and C_2 are constants calculated from the initial values of A_1 and A_2.

When a change of $\kappa(z)$ larger than 0.1% occurred, we chose a smaller layer and calculated the new corresponding set of values of constants for the corresponding layer Δz. We started evaluating the initial set of constants for the first layer at the surface of the sample by using $\kappa(z = 0) = \kappa_0$. Next, for the following layers, the values of the complex amplitudes of the beams at the end of each interval were used to evaluate m and therefore we obtain a new value of κ at z where the following layer starts.

From the complex amplitudes, obtained from the self-consistent solutions of the set of equations, we calculated the intensities and phases of each wave. From these we calculated the corresponding light modulation $m(z)$ as a function of z, for each sample of thickness d.

Then, with the previously recorded Δn$_1(z)$, we calculated the diffraction efficiency

$$\eta = \frac{I_{diff}}{I_{trans} + I_{diff}}. \tag{20}$$

Where I_{trans} and I_{diff} are the transmitted and diffracted intensities respectively. The grating can be read from the left or from the right side (see Fig. 1). The values for the diffraction efficiency for these two Bragg-matched conditions can

be different when phase and amplitude gratings are simultaneously present [16]. We calculated the diffraction efficiency reading from the left (η_L) and from the right side (η_R). This was done exchanging the solutions for A_1 and A_2 given in Eqs. (18) and (19), and applying Eq. (20).

4. Results and discussion

Our calculations were performed for the Bragg condition, with a wavelength $\lambda = 488$ nm. We used several values for the fringe spacing, Λ = 1.0; 0.420 and 0.250 microns, and an applied d.c. field of 5 Kv/cm.

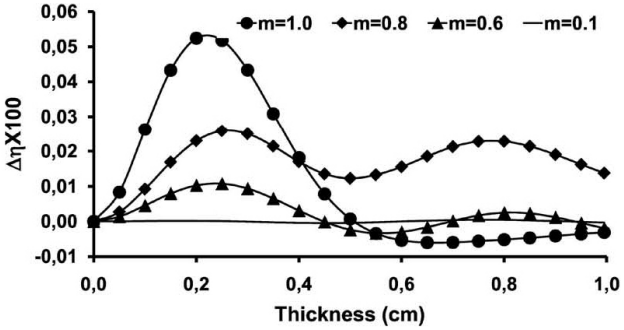

FIGURE 2. Difference of the values for the diffraction efficiency amplified 100 times. The fringe spacing is Λ = 0.105 microns. The applied field is 5 Kv/cm.

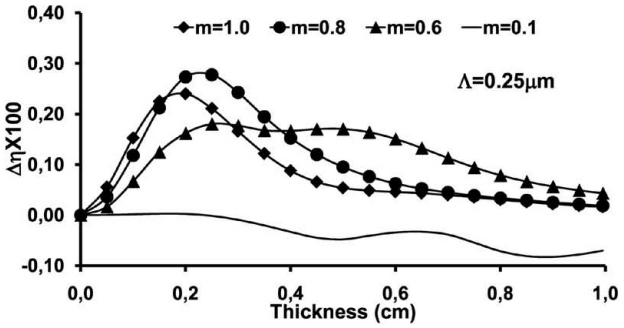

FIGURE 3. Difference of the values for the diffraction efficiency amplified 100 times. The fringe spacing is Λ = 0.250 microns. The applied field is 5 Kv/cm.

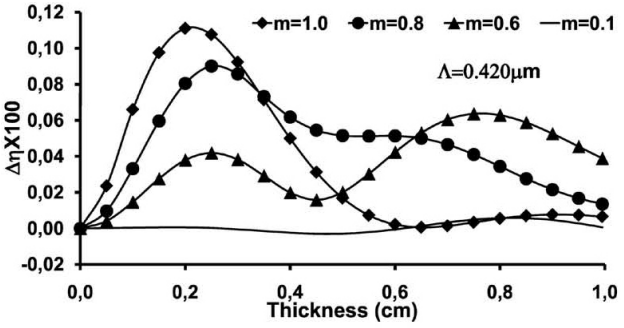

FIGURE 4. Difference of the values for the diffraction efficiency amplified 100 times. The fringe spacing is Λ = 0.420 microns. The applied field is 5 Kv/cm.

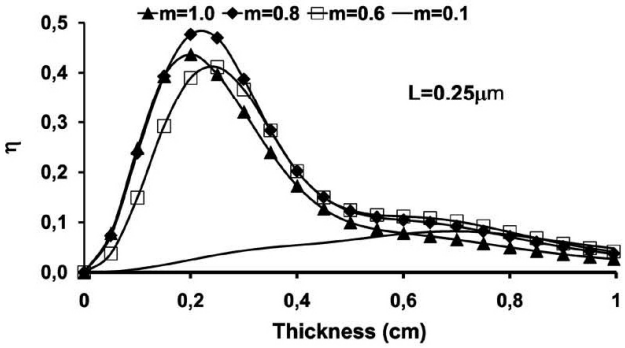

FIGURE 5. Total diffraction efficiency as a function of sample thickness. We show the value of η for Λ = 0.250 micron and simultaneous phase and absorption gratings.

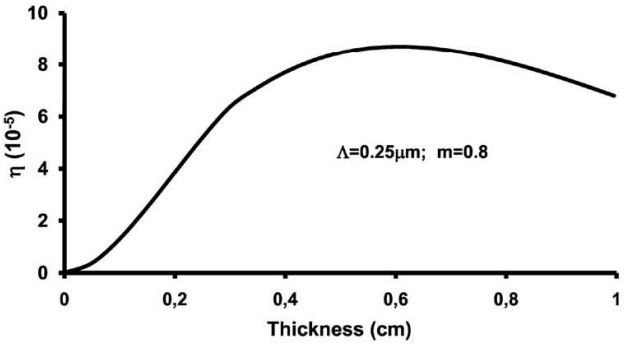

FIGURE 6. Calculation of the diffraction efficiency due to the absorption grating alone.

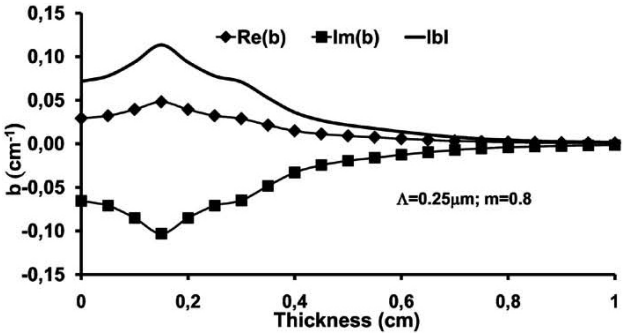

FIGURE 7. The coupling parameter due to the absorption grating, b, as a function of sample thickness. We show the variation of the real part, of the imaginary part and of the magnitude of b. From this figure, we see clearly that the phase, φ_a, of the absorption coefficient is different from zero. The fringe spacing is Λ=0.250 microns. The applied field is 5 Kv/cm, and m_0= 0.8.

In Figs. 2 to 4 we show the difference of the values for the diffraction efficiency amplified 100 times. We did this for several values of the incident light modulation and grating period. We can see that this difference is very small for all cases. The largest values for this difference occur for a grating of 0.250 microns (see Figs. 3).

In Fig. 5 we show the value of the diffraction efficiency, for Λ = 0.250 microns and simultaneous phase and absorption gratings. For this case, the largest difference between the two

values of the diffraction efficiency is around 5×10^{-3}. This difference cannot be seen on this figure.

In Fig. 6 we show the diffraction efficiency for the absorption grating alone, with Λ = 0.250 microns and m_0=0.8. The largest value is around 10^{-4} and occurs for a sample thickness of about 0.8 cm.

Finally, in Fig. 7 we show the real, the imaginary part and the magnitude of the complex absorption coefficient [see Eqs. (16) and (17)]. From this figure, we can see clearly that the phase of the absorption modulation is not zero.

5. Summary and conclusions

For the transmission geometry, we have considered the simultaneous presence of phase and absorption gratings of iron doped lithium niobate. In order to assess the importance of the absorption grating on the total value of the diffraction efficiency, we followed several steps. The first was to solve numerically the set of nonlinear differential equation for the material using the band transport model from 0 seconds up to the stationary state. We included the photovoltaic effect. From the solution, we obtained the full space charge field and the final donor density. Then we performed the Fourier decomposition for each of the calculated overall space charge fields. In this way, we obtained the amplitude E_1 of its fundamental component and its phase, Φ_G, with regard to the light interference pattern. We did this for several values of m between 0 and 1. In all cases, we included an applied field of 5 kV/cm. The modulation of the absorption coefficient depends on the magnitude of the first Fourier coefficient of the concentration of ionized donors. The corresponding phase is not zero. These solutions were used to include the non uniformity of the gratings to calculate the beam energy exchange.

Then, we solved the beam coupling equations for recording and for reading in a self-consistent way to include the variation of light modulation along the sample thickness. From these solutions, we calculated the beam intensities, the light modulation and diffraction efficiency when both gratings are present, and with only the phase grating. We found that the contribution of the absorption grating to the value of the diffraction efficiency, for the given set of values for physical parameters of $LiNbO_3$ is negligible. The contribution of the absorption grating is less than 0.5% of the total value of the diffraction efficiency. The value of the modulation of the absorption coefficient depends on the magnitude of the first Fourier coefficient of the concentration of ionized donors in the material for the stationary state. The phase of the absorption coefficient modulation is not zero.

Acknowledgements

We thank Dirección General de Asuntos del Personal Académico for partial funding by the grant IN111807.

∗. Phone: +[52]5556225122; FAX: +[52]5556225011; e-mail: fernando@fisica.unam.mx

1. K. Buse, A. Adibi, and D. Psaltis, *Nature* **393** (1998) 665.
2. V.M. Petrov, S. Lichtenberg, A.V. Chamrai, J. Petter, and T. Tschudi, *Thin solid Films* **450** (2004) 178.
3. P. Arora, V.M. Petrov, J. Petter, and T. Tschudi, *Optics Communications* **281** (2008) 1455.
4. M. Luennemann, K. Buse, and B. Sturman, *Journal of Applied Physics* **94** (2003) 6274.
5. P. Arora, V.M. Petrov, J. Petter, and T. Tschudi, *Optics Communications* **278** (2007) 423.
6. L. Solymar, D.J. Webb, and A. Grunnet-Jepsen, *Calderon Press* (Oxford 1996) p. 22
7. K. Buse, *Appl. Phys. B* **64** (1997) 273.
8. S. Stepanov, and C. Nuñez-Santiago, *Optics Communications* **264** (2006) 105.
9. L.F. Magaña, I. Casar, and J.G. Murillo, *Opt. Mater.* **30** (2008) 979.
10. N.V. Kukhtarev, V.B. Markov, S.G. Odulov, M.S. Soskin, and V.L. Vinetskii, *Ferroelectrics* **22** (1979) 961.
11. M. Saffman, D. Montgomery, A.A. Zozulya, K. Kuroda, and D.Z. Ardenson, *Phys. Rev* **48** (1993) 3209.
12. G.W. Burr and D. Psaltis, *Opt. Lett.* **21** (1996) 893.
13. J.G. Murillo, L.F. Magaña, M. Carrascosa, and F. Agulló-López, *J. Opt Soc. Am. B* **15** (1998) 2092.
14. J.G. Murillo, L.F. Magaña, M. Carrascosa, and F. Agulló-López, *J. Appl. Phys.* **78** (1995) 5686.
15. P. Yeh, *Introduction to photorefractive nonlinear optics* (John Wiley & Sons, Inc. New York, NY, 1993) p.264
16. E. Guibelalde, *Opt. Quantum Electron.* **16** (1984) 173.